Inorg. Chem. **2009**, *48*, 2010−2017

Inorganic Chemistry

Article

Lanthanide−Organic Cation Frameworks with Zeolite Gismondine Topology and Large Cavities from Intersected Channels Templated by Polyoxometalate Counterions

Chun-Hong Li,[†] Kun-Lin Huang,[‡] Ying-Nan Chi,[†] Xi Liu,[‡] Zhan-Gang Han,[†] Long Shen,[†] and Chang-Wen Hu*[,†]

Department of Chemistry, The Institute for Chemical Physics, and State Key Laboratory of Explosion Science and Technology, Beijing Institute of Technology, Beijing 100081, China, and College of Chemistry, Chongqing Normal University, Chongqing 400047, China

Received September 29, 2008

A family of organic−inorganic hybrid frameworks, $\{[Ln(H_2O)_4(pdc)]_4\}$ $[XMo_{12}O_{40}]\cdot 2H_2O$ (Ln = La, Ce, and Nd; X = Si and Ge; H_2pdc = pyridine-2,6-dicarboxylate), have been prepared under hydrothermal conditions and characterized by single crystal X-ray diffraction analyses, elemental analyses, IR, and thermal gravimetric analyses. Single crystal X-ray diffraction reveals that all six compounds are isostructural, and each consists of a zeolite-like four-connected three-dimensional cationic framework $\{[Ln(H_2O)_4(pdc)]_4\}^{4+}$ and ball-shaped Keggin type $[XMo_{12}O_{40}]^{4-}$ as templates. Interesting channels exist in the cationic framework with the gismondine topology, and these channels intersect each other to form large cavities, which array in a zigzag fashion and are occupied by nanosized $[XMo_{12}O_{40}]^{4-}$ counterions. Moreover, these compounds display strong photoluminescent properties in the solid state at room temperature.

Introduction

The study of metal−organic frameworks (MOFs) is developing rapidly because of not only their intriguing structural diversity but also their potential applications in molecular adsorption, ion exchange, and heterogeneous catalysis, as well as electrical, magnetic, and photochemical areas.[1] For the construction of MOFs, polyoxometalates (POMs), as one kind of significant metal oxide cluster with nanosizes, have often been employed as inorganic counter-anions, and the strategy of supramolecular assembly was extensively developed.[2] Besides balancing charge, POMs can act as anionic templates to build POM-based cationic MOFs due to their controllable shape and size.[3−5]

Prior to now, a number of novel architectures resulting from the incorporation of POMs and organic ligands have been reported, including several three-dimensional (3D) POM-templated MOFs from neutral N-donor ligands and transitional metal elements,[6,7] but the rational synthesis of

---

* To whom correspondence should be addressed. E-mail: cwhu@bit.edu.cn. Fax: +86-10-68914780.

[†] Beijing Institute of Technology.

[‡] Chongqing Normal University.

(1) (a) Lu, W. G.; Jiang, L.; Feng, X. L.; Lu, T. B. *Cryst. Growth Des.* **2008**, *8*, 986, and references cited therein. (b) Wang, Y. T.; Fan, H. H.; Wang, H. Z.; Chen, X. M. *Inorg. Chem.* **2005**, *44*, 4148. (c) Chen, B.; Ji, Y.; Xue, M.; Fronczek, F. R.; Hurtado, E. J.; Mondal, J. U.; Liang, C.; Dai, S. *Inorg. Chem.* **2008**, *47*, 5543. (d) Chen, B.; Wang, L.; Zapata, F.; Qian, G.; Lobkovsky, E. B. *J. Am. Chem. Soc.* **2008**, *130*, 6718. (e) Ma, L.; Lee, J. Y.; Li, J.; Lin, W. *Inorg. Chem.* **2008**, *47*, 3955. (f) Cheng, J. W.; Zheng, S. T.; Ma, E.; Yang, G. Y. *Inorg. Chem.* **2007**, *46*, 10534.

(2) (a) Coronado, E.; Gómez-García, C. J. *Chem. Rev.* **1998**, *98*, 273. (b) Hagrman, P. J.; Hagrman, D.; Zubieta, J. *Angew. Chem., Int. Ed.* **1999**, *38*, 2638. (c) Han, Z.; Gao, Y.; Hu, C. *Cryst. Growth Des.* **2008**, *8*, 1261.

(3) (a) Wang, X.; Bi, Y.; Chen, B.; Lin, H.; Liu, G. *Inorg. Chem.* **2008**, *47*, 2442. (b) Hagrman, D.; Zubieta, J. *Chem. Commun.* **1998**, 2005. (c) Zheng, L. M.; Wang, Y. S.; Wang, X. Q.; Korp, J. D.; Jacobson, A. J. *Inorg. Chem.* **2001**, *40*, 1380. (d) Inman, C.; Knaust, J. M.; Keller, S. W. *Chem. Commun.* **2002**, 156.

(4) (a) Ren, Y. P.; Kong, X. J.; Hu, X. Y.; Sun, M.; Long, L. S.; Huang, R. B.; Zheng, L. S. *Inorg. Chem.* **2006**, *45*, 4016. (b) Jin, H.; Qi, Y. F.; Wang, E. B.; Li, Y. G.; Wang, X. L.; Qin, C.; Chang, S. *Eur. J. Inorg. Chem.* **2006**, *4541*, 4545. (c) Wei, M.; He, C.; Hua, W.; Duan, C.; Li, S.; Meng, Q. *J. Am. Chem. Soc.* **2006**, *128*, 13318.

(5) (a) Uehara, K.; Kasai, K.; Mizuno, N. *Inorg. Chem.* **2007**, *46*, 2563. (b) Li, Y. G.; Dai, L. M.; Wang, Y. H.; Wang, X. L.; Wang, E. B.; Su, Z. M.; Xu, L. *Chem. Commun.* **2007**, 2593. (c) Sun, C. Y.; Li, Y. G.; Wang, E. B.; Xiao, D. R.; An, H. Y.; Xu, L. *Inorg. Chem.* **2007**, *46*, 1563. (d) Wei, M. L.; He, C.; Sun, Q. Z.; Meng, Q. J.; Duan, C. Y. *Inorg. Chem.* **2007**, *46*, 5957.

(6) (a) Zheng, L. M.; Whitfield, T.; Wang, X.; Jacobson, A. J. *Angew. Chem., Int. Ed.* **2000**, *39*, 4528. (b) Lü, J.; Shen, E. H.; Yuan, M.; Li, Y. G.; Wang, E. B.; Hu, C. W.; Xu, L.; Peng, J. *Inorg. Chem.* **2003**, *42*, 6956.

10.1021/ic801846h CCC: $40.75

Table 1. Crystallographic Data for Compounds **1**−**6**

	1	**2**	**3**	**4**	**5**	**6**
formula	$C_{28}H_{48}La_4SiMo_{12}N_4O_{74}$	$C_{28}H_{48}Ce_4SiMo_{12}N_4O_{74}$	$C_{28}H_{48}Nd_4SiMo_{12}N_4O_{74}$	$C_{28}H_{48}La_4GeMo_{12}N_4O_{74}$	$C_{28}H_{48}Ce_4GeMo_{12}N_4O_{74}$	$C_{28}H_{48}Nd_4GeMo_{12}N_4O_{74}$
fw	3359.71	3364.55	3381.03	3404.23	3409.07	3425.55
a (Å)	30.863(3)	30.753(3)	30.514(3)	30.846(3)	30.727(3)	30.573(3)
b (Å)	15.7425(16)	15.7285(13)	15.6715(19)	15.7730(17)	15.769(2)	15.733(2)
c (Å)	22.192(2)	22.119(2)	22.003(2)	22.189(2)	22.110(2)	22.013(3)
α (deg)	90	90	90	90	90	90
β (deg)	133.173(1)	133.118(1)	133.025(2)	133.134(2)	133.080(1)	132.965(2)
γ (deg)	90	90	90	90	90	90
space group	$C2/c$	$C2/c$	$C2/c$	$C2/c$	$C2/c$	$C2/c$
D_{calcd} (g cm^{-3})	2.838	2.862	2.920	2.870	2.894	2.937
Z	4	4	4	4	4	4
crystal system	monoclinic	monoclinic	monoclinic	monoclinic	monoclinic	monoclinic
volume (Å^3)	7863.4(13)	7809.7(12)	7692.1(14)	7878.2(14)	7824.8(14)	7748.3(17)
M	4.107	4.279	4.677	4.459	4.632	5.008
F(000)	6328.0	6344.0	6376.0	6400.0	6416.0	6448.0
reflns collected	19616	19414	19646	23695	19512	18684
unique reflns	6920	6877	6760	9225	6889	6836
GOF	1.002	1.000	1.007	1.004	1.006	1.002
R_{int}	0.0255	0.0309	0.0377	0.0318	0.0321	0.0413
R_1 [$I > 2\sigma(I)$]	0.0833	0.0847	0.0813	0.0819	0.0762	0.0752
wR_2 [$I > 2\sigma(I)$]	0.2826	0.1901	0.1756	0.1718	0.1468	0.1599
R_1 (all data)[a]	0.1068	0.1250	0.1263	0.1297	0.1216	0.1177
wR_2 (all data)[b]	0.3042	0.2072	0.1927	0.1891	0.1608	0.1759

[a] $R_1 = \sum||F_o| - |F_c||/\sum|F_o|$. [b] $wR_2 = \sum[w > (F_o^2 - F_c^2)^2]/\sum[w > (F_o^2)^2]^{1/2}$.

high-connected 3D POM-based MOFs is still one of the great challenges,[8,9] so rare earth elements and O-donor organic ligands are seldom adopted.[10]

It is well known that the oxygen atoms on the surface of POMs are rather reactive. Some of the highly oxophilic rare earth ions can readily incorporate with POMs and O-donor organic ligands, so in most cases they only precipitate instead of crystallize.[11] Recent elaboration has proven that the hydrothermal technique is an effective approach for the preparation of higher-dimensional hybrid materials.[12,13] Therefore, one-pot hydrothermal synthesis provides an alternative way to solve the above-mentioned fast precipitation process.[14] In this work, we successfully achieved a family of 3D POM-based lanthanide−organic coordination polymers, formulated as $\{[Ln(H_2O)_4(pdc)]_4\}[XMo_{12}O_{40}]\cdot 2H_2O$ (Ln = La, Ce, and Nd; X = Si for **1**−**3** and Ge for **4**−**6**, respectively; H_2pdc = pyridine-2,6-dicarboxylate). All these compounds are isostructural, and each displays a four-connected 3D cationic network with zeolite-like gismondine (GIS) topology and the ball-shaped Keggin type polyoxoanions $[XMo_{12}O_{40}]^{4-}$ (X = Ge, Si) as templates. To the best of our knowledge, lanthanide−organic coordination polymers with zeolite-like GIS topology have not been reported to date. Furthermore, these compounds represent the first examples in which large cavities from intersected channels of a rare-earth−organic complex are occupied by the saturated heteropolyoxoanions.

Experimental Section

General Considerations. All chemicals were commercially purchased and used without further purification. Infrared spectra were obtained (as KBr pressed pellets) using a Nicolet 170SXFT/IR spectrometer. X-ray powder diffraction (XPRD) of samples were collected on a Japan Rigaku D/max γA X-ray diffractometer equipped with graphite monochromatized Cu Kα radiation (λ = 0.154060 nm). The C, H, and N elemental analyses were performed on Perkin-Elmer 2400 CHN elemental analyzer. Fluorescence spectra were performed on a Hitachi F-4500 fluorescence/phosphorescence spectrophotometer. Thermal gravimetric (TG) analyses were carried out in a nitrogen atmosphere between 50 and 800 °C at a heating rate of 10 °C/min on a ZRY-2P simultaneous thermal analyzer.

Synthesis of Compound 1. A mixture of H_2pdc (0.1 mmol, 16.7 mg), $Na_2MoO_4\cdot 2H_2O$ (0.1 mmol, 24.2 mg), $La(NO_3)_3\cdot 6H_2O$ (0.1 mmol, 43.3 mg), $Na_2SiO_3\cdot 9H_2O$ (0.1 mmol, 28.4 mg), and H_2O (8 mL) with a starting pH of 2.0 adjusted with 1 mol L^{-1} HCl was sealed in a 15 mL Teflon lined stainless steel container and heated at 100 °C for 72 h under autogenous pressure. After cooling to room temperature, yellow cubic crystals were collected for X-ray analysis. Yield: 46% (based on Mo). Anal. Calcd for $C_{28}H_{48}La_4SiMo_{12}N_4O_{74}$: C, 10.00; H, 1.43; N, 1.67%. Found: C, 10.06; H, 1.38; N, 1.61%. IR (KBr, cm^{-1}) ν: 3430 (s), 1621 (s), 1565 (s), 1443 (s), 1386 (s), 1282 (m), 1195 (w), 1078 (m), 1021 (w), 991 (w), 956 (s), 908 (vs), 800 (vs), 765 (vs), 700 (w), 669 (w), 586 (w), 534 (w).

Synthesis of Compound 2. The synthetic procedure was similar to that of **1** except that $Ce(NO_3)_3\cdot 6H_2O$ was used instead of $La(NO_3)_3\cdot 6H_2O$. Yellow cubic crystals were obtained in about 33% yield based on Mo. Anal. Calcd for $C_{28}H_{48}Ce_4SiMo_{12}N_4O_{74}$: C, 9.99; H, 1.43; N, 1.66%. Found: C, 10.02; H, 1.38; N, 1.61%. IR (KBr,

---

(7) (a) Li, Y. G.; De, G.; Yuan, M.; Wang, E. B.; Huang, R. D.; Hu, C. W.; Hu, N. H.; Jia, H. Q. *Dalton Trans.* **2003**, 334. (b) Feng, S. H.; Xu, R. R. *Acc. Chem. Res.* **2001**, *34*, 239.

(8) (a) Kong, X. J.; Ren, Y. P.; Zheng, P. Q.; Long, Y. X.; Long, L. S.; Huang, R. B.; Zheng, L. S. *Inorg. Chem.* **2006**, *45*, 10702. (b) Turro, N. *Acc. Chem. Res.* **2000**, *33*, 637.

(9) (a) Pan, L.; Liu, H. M.; Lei, X. G.; Huang, X. Y.; Olson, D. H.; Turro, N. J.; Li, J. *Angew. Chem., Int. Ed.* **2003**, *42*, 542. (b) Eddaoudi, M.; Moler, D. B.; Li, H. L.; Chen, B. L.; Reineke, T. M.; O'Keeffe, M.; Yaghi, O. M. *Acc. Chem. Res.* **2001**, *34*, 319.

(10) (a) Zhang, H.; Duan, L.; Lan, Y.; Wang, E.; Hu, C. *Inorg. Chem.* **2003**, *42*, 8053. (b) Mialane, P.; Dolbecq, A.; Lisnard, L.; Mallard, A.; Marrot, J.; Sécheresse, F. *Angew. Chem., Int. Ed.* **2002**, *41*, 2398.

(11) Wu, C. D.; Lu, C. Z.; Zhuang, H. H.; Huang, J. S. *J. Am. Chem. Soc.* **2002**, *124*, 3836.

(12) (a) Liu, C. M.; Zhang, D. Q.; Zhu, D. B. *Cryst. Growth Des.* **2006**, *6*, 524. (b) Lu, J. Y.; Lawandy, M. L.; Li, J.; Yuen, T.; Lin, C. L. *Inorg. Chem.* **1999**, *38*, 2695.

(13) (a) Rabenau, A. *Angew. Chem., Int. Ed. Engl.* **1985**, *24*, 1026. (b) Ludise, R. A. *Chem. Eng. News* **1987**, *65*, 30. (c) Gopalakrishnan, J. *Chem. Mater.* **1995**, *7*, 1265.

(14) (a) Soghomonian, V.; Chen, Q.; Haushalter, R.; Zubieta, J. *Chem. Mater.* **1993**, *5*, 1595. (b) Cui, X. B.; Xu, J. Q.; Meng, H.; Zheng, S. T.; Yang, G. Y. *Inorg. Chem.* **2004**, *43*, 8005.

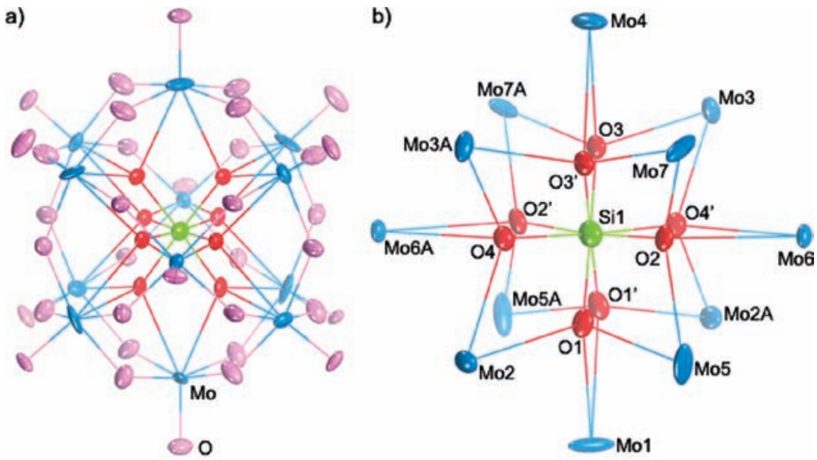

Figure 1. (a) Crystal structure of $[SiMo_{12}O_{40}]^{4-}$. (b) Disorder of SiO_4.

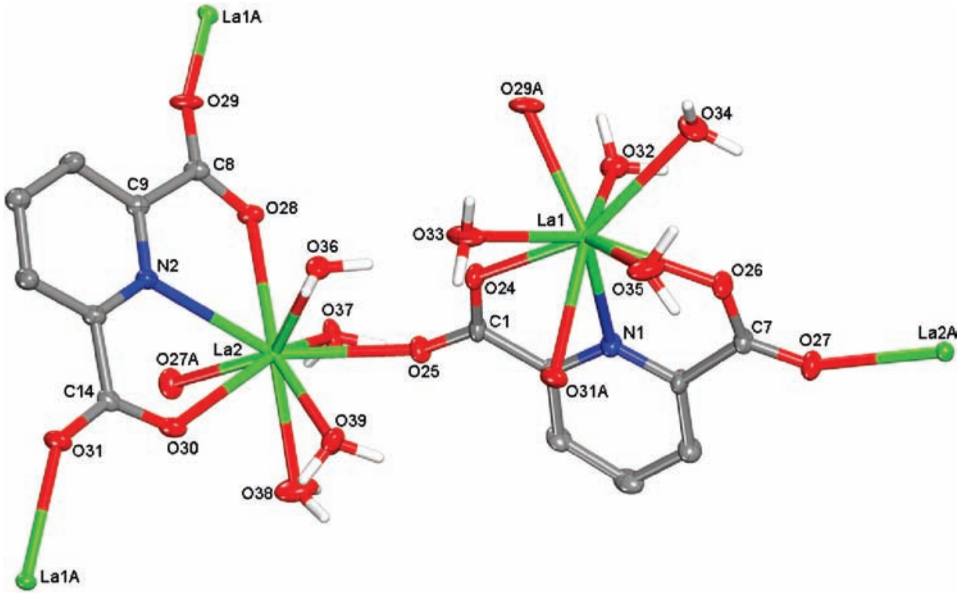

Figure 2. Coordination mode of two crystallographically independent La centers.

cm^{-1}) ν: 3426 (s), 1621 (s), 1565 (s), 1443 (s), 1386 (s), 1282 (m), 1195 (w), 1078 (m), 1021 (w), 991 (w), 956 (s), 908 (vs), 800 (vs), 765 (vs), 700 (w), 669 (w), 586 (w), 534 (w).

Synthesis of Compound 3. The synthetic procedure was similar to that of **1** except that $Nd(NO_3)_3 \cdot 6H_2O$ was used instead of $La(NO_3)_3 \cdot 6H_2O$. Yellow cubic crystals were obtained in about 39% yield based on Mo. Anal. Calcd for $C_{28}H_{48}Nd_4SiMo_{12}N_4O_{74}$: C, 9.94; H, 1.42; N, 1.66%. Found: C, 9.98; H, 1.36; N, 1.60%. IR (KBr, cm^{-1}) ν: 3430 (s), 1621 (s), 1565 (s), 1443 (s), 1386 (s), 1282 (m), 1195 (w), 1078 (m), 1021 (w), 991 (w), 956 (s), 908 (vs), 800 (vs), 765 (vs), 700 (w), 669 (w), 586 (w), 534 (w).

Synthesis of Compound 4. A mixture of H_2pdc (0.1 mmol, 16.7 mg), $Na_2MoO_4 \cdot 2H_2O$ (0.1 mmol, 24.2 mg), $La(NO_3)_3 \cdot 6H_2O$ (0.1 mmol, 43.3 mg), GeO_2 (0.1 mmol, 10.5 mg), and H_2O (8 mL) with a starting pH of 2.0 adjusted with 1 mol L^{-1} HCl was sealed in a 15 mL Teflon lined stainless steel container and heated at 100 °C for 72 h under autogenous pressure. After cooling to room temperature, yellow cubic crystals were collected for X-ray analysis. Yield: 51% (based on Mo). Anal. Calcd for $C_{28}H_{48}La_4GeMo_{12}N_4O_{74}$: C, 9.87; H, 1.41; N, 1.65%. Found: C, 9.92; H, 1.43; N, 1.68%. IR (KBr, cm^{-1}) ν: 3417 (s), 1621 (s), 1565 (s), 1443 (s), 1386 (s), 1282 (m), 1195 (w), 1078 (m), 1021 (w), 960 (s), 886 (vs), 808 (m), 786 (m), 769 (vs), 700 (w), 669 (w), 591 (w), 508 (w).

Synthesis of Compound 5. The synthetic procedure was similar to that of **4** except that $Ce(NO_3)_3 \cdot 6H_2O$ was used instead of $La(NO_3)_3 \cdot 6H_2O$. Yellow cubic crystals were obtained in about 28% yield based on Mo. Anal. Calcd for $C_{28}H_{48}Ce_4GeMo_{12}N_4O_{74}$: C, 9.86; H, 1.41; N, 1.64%. Found: C, 9.91; H, 1.37; N, 1.60%. IR (KBr, cm^{-1}) ν: 3417 (s), 1621 (s), 1565 (s), 1443 (s), 1386 (s), 1282 (m), 1195 (w), 1078 (m), 1021 (w), 960 (s), 886 (vs), 808 (m), 786 (m), 769 (vs), 700 (w), 669 (w), 591 (w), 508 (w).

Synthesis of Compound 6. The synthetic procedure was similar to that of **4** except that $Nd(NO_3)_3 \cdot 6H_2O$ was used instead of $La(NO_3)_3 \cdot 6H_2O$. Yellow cubic crystals were obtained in about 28% yield based on Mo. Anal. Calcd for $C_{28}H_{48}Nd_4GeMo_{12}N_4O_{74}$: C, 9.81; H, 1.40; N, 1.63%. Found: C, 9.86; H, 1.34; N, 1.59%. IR (KBr, cm^{-1}) ν: 3417 (s), 1621 (s), 1565 (s), 1443 (s), 1386 (s), 1282 (m), 1195 (w), 1078 (m), 1021 (w), 960 (s), 886 (vs), 808 (m), 786 (m), 769 (vs), 700 (w), 669 (w), 591 (w), 508 (w).

X-ray Crystallographic Analysis. The structures of compounds **1**−**6** were determined by a Bruker-AXS CCD diffractometer equipped with a graphite-monochromated Mo Kα radiation source

Table 2. Selected Bond Distances (Å) and Angles (deg) of **1**[a]

	Distances (Å)		
La(1)−O(29)$^{\#1}$	2.487(13)	La(1)−O(26)	2.505(13)
La(1)−O(24)	2.528(13)	La(1)−O(33)	2.531(13)
La(1)−O(35)	2.585(15)	La(1)−O(31)$^{\#2}$	2.580(12)
La(1)−N(1)	2.634(13)	La(1)−O(34)	2.668(15)
La(1)−O(32)	2.659(14)	La(2)−O(27)$^{\#3}$	2.470(12)
La(2)−O(25)	2.515(11)	La(2)−O(38)	2.535(14)
La(2)−O(28)	2.523(12)	La(2)−O(30)	2.572(12)
La(2)−O(37)	2.559(13)	La(2)−O(39)	2.613(12)
La(2)−O(36)	2.644(12)	La(2)−N(2)	2.640(14)
	Angles (deg)		
O(29)$^{\#1}$−La(1)−O(26)	134.2(5)	O(29)$^{\#1}$−La(1)−O(24)	87.2(5)
O(26)−La(1)−O(24)	123.5(4)	O(29)$^{\#1}$−La(1)−O(33)	68.1(4)
O(26)−La(1)−O(33)	146.1(5)	O(24)−La(1)−O(33)	74.7(5)
O(29)$^{\#1}$−La(1)−O(31)$^{\#2}$	137.7(4)	O(26)−La(1)−O(31)$^{\#2}$	85.9(5)
O(24)−La(1)−O(31)$^{\#2}$	76.7(5)	O(33)−La(1)−O(31)$^{\#2}$	69.9(4)
O(29)$^{\#1}$−La(1)−O(35)	109.6(5)	O(26)−La(1)−O(35)	69.4(5)
O(24)−La(1)−O(35)	140.8(5)	O(33)−La(1)−O(35)	79.2(5)
O(31)$^{\#2}$−La(1)−O(35)	67.0(5)	O(29)$^{\#1}$−La(1)−N(1)	136.7(4)
O(26)−La(1)−N(1)	62.6(4)	O(24)−La(1)−N(1)	61.1(4)
O(33)−La(1)−N(1)	123.1(5)	O(31)$^{\#2}$−La(1)−N(1)	66.6(4)
O(35)−La(1)−N(1)	113.6(4)	O(29)$^{\#1}$−La(1)−O(32)	72.5(4)
O(26)−La(1)−O(32)	83.3(5)	O(24)−La(1)−O(32)	74.6(5)
O(33)−La(1)−O(32)	130.5(5)	O(31)$^{\#2}$−La(1)−O(32)	136.5(4)
O(35)−La(1)−O(32)	143.5(5)	N(1)−La(1)−O(32)	71.0(5)
O(29)$^{\#1}$−La(1)−O(34)	69.0(5)	O(26)−La(1)−O(34)	66.9(5)
O(24)−La(1)−O(34)	144.3(5)	O(33)−La(1)−O(34)	116.8(5)
O(31)$^{\#2}$−La(1)−O(34)	138.5(5)	O(35)−La(1)−O(34)	74.1(5)
N(1)−La(1)−O(34)	120.1(4)	O(32)−La(1)−O(34)	73.1(5)
O(27)$^{\#3}$−La(2)−O(25)	136.6(4)	O(27)$^{\#3}$−La(2)−O(28)	83.1(5)
O(25)−La(2)−O(28)	98.2(4)	O(27)$^{\#3}$−La(2)−O(38)	70.6(5)
O(25)−La(2)−O(38)	83.4(5)	O(28)−La(2)−O(38)	141.3(5)
O(27)$^{\#3}$−La(2)−O(37)	73.0(4)	O(25)−La(2)−O(37)	66.7(4)
O(28)−La(2)−O(37)	71.1(4)	O(38)−La(2)−O(37)	74.3(5)
O(27)$^{\#3}$−La(2)−O(30)	76.7(4)	O(25)−La(2)−O(30)	133.3(4)
O(28)−La(2)−O(30)	121.2(4)	O(38)−La(2)−O(30)	80.4(5)
O(37)−La(2)−O(30)	145.5(4)	O(27)$^{\#3}$−La(2)−O(39)	129.3(5)
O(25)−La(2)−O(39)	68.0(4)	O(28)−La(2)−O(39)	145.3(4)
O(38)−La(2)−O(39)	71.0(5)	O(37)−La(2)−O(39)	124.9(4)
O(30)−La(2)−O(39)	65.4(4)	O(27)$^{\#3}$−La(2)−N(2)	73.8(4)
O(25)−La(2)−N(2)	143.6(4)	O(28)−La(2)−N(2)	60.4(4)
O(38)−La(2)−N(2)	132.2(5)	O(37)−La(2)−N(2)	123.4(4)
O(30)−La(2)−N(2)	61.0(4)	O(39)−La(2)−N(2)	111.7(4)
O(27)$^{\#3}$−La(2)−O(36)	147.4(4)	O(25)−La(2)−O(36)	72.3(4)
O(28)−La(2)−O(36)	76.7(4)	O(38)−La(2)−O(36)	138.4(5)
O(37)−La(2)−O(36)	122.3(4)	O(30)−La(2)−O(36)	92.1(4)
O(39)−La(2)−O(36)	68.8(4)	N(2)−La(2)−O(36)	74.1(4)

[a] Symmetry codes for **1**: (#1) $-x + 1$, y, $-z + 3/2$; (#2) $-x + 1/2$, $-y + 3/2$, $-z + 1$; (#3) x, $-y + 1$, $z - 1/2$.

($\lambda = 0.71073$ Å) at 298 K. All absorption corrections were performed with the SADABS program. All the structures were solved by direct methods and expanded using Fourier techniques. The nonhydrogen atoms were refined anisotropically. Hydrogen atoms were located in the calculated positions. All calculations were performed using the SHELXTL-97 program.[15] The crystallographic details of **1**−**6** are summarized in Table 1. Crystallographic data for the structures reported in this paper have been deposited in the Cambridge Crystallographic Data Center with CCDC reference numbers 692103−692108 for compounds **1**−**6**, respectively.

Results and Discussion

Synthesis and IR Spectroscopy. Syntheses of compounds **1**−**6** were achieved by the hydrothermal technique. The formation of products is not significantly affected by changes of the reaction mole ratio of the materials. Many parallel experiments prove that the quality of crystals depends on the temperature, and the optimal temperature is 100 °C. The resultant crystals are stable in air and insoluble in water or common organic solvents.

In the IR spectrum of compound **1**, the characteristic peaks at 956, 908, 800, and 765 cm^{-1} are attributed to the Keggin polyoxoanion. The absence of strong peaks around 1720 cm^{-1} indicates that all carboxylic groups are deprotonated.[16] The peaks of the carboxylic groups are at 1621 and 1565 cm^{-1} for the asymmetric stretching and 1443 cm^{-1} for the symmetric stretching. The separations (Δ) between $\nu_{\mathrm{asym}}(\mathrm{CO_2})$ and $\nu_{\mathrm{sym}}(\mathrm{CO_2})$ are at 178 and 122 cm^{-1}, which are attributed to the existence of both the bridging and the chelate modes of the carboxylate groups, respectively.[17] Similar IR characteristics have been observed for compounds **2**−**6**.

Description of Crystal Structures. X-ray analysis shows that all six compounds are isostructural. As an example, compound **1** was described here and consists of a noncoordinated $[\mathrm{SiMo_{12}O_{40}}]^{4-}$ anion, four $[\mathrm{La(H_2O)_4(pdc)}]^{+}$ cations, and two crystalline water molecules. The polyoxoanion structure of **1** is displayed in Figure 1a. In this case, the well-known Keggin core is unexceptional, consisting of a central $\mathrm{SiO_4}$ tetrahedron surrounded by 12 $\mathrm{MoO_6}$ octahedra arranged in four groups of three edge-sharing octahedral subunits $\mathrm{Mo_3O_{13}}$. Each trinuclear subunit is in turn linked by the corner that they share and to the central $\mathrm{SiO_4}$ tetrahedron. In Figure 1b, the central Si atom is surrounded by a distorted cube constituted by eight half-occupied oxygen atoms. The structure feature of disorder often appears in the Keggin structure.[18]

Figure 2 displays the coordination mode of two crystallographically independent La centers (La1 and La2) with similar coordination environments. The nine-coordinated $\mathrm{La^{3+}}$ center coordinates to one nitrogen atom of pdc ligand, four oxygen atoms of the carboxyl groups of three different pdc ligands, and four water molecules. Each pdc ligand adopts an exo-tridentate coordination fashion. The bond length of La1−O is different from that of La2−O (Table 2). The average La1−O(water) distance is 2.611 Å, which is longer than the average La1−O(pdc) distance of 2.525 Å. The average La2−O(water) distance is 2.588 Å, which is also longer than the average La2−O(pdc) distance of 2.520 Å. The La(III)−O and La(III)−N distances are similar to those found in other La(III) complexes.[19]

In compound **1**, three interesting structure features exist: (i) $[\mathrm{SiMo_{12}O_{40}}]^{4-}$ ions chelated by two $\mathrm{La_4}$ clusters via

---

(15) (a) Sheldrick, G. M. *SHELXS 97, Program for Crystal Structure Solution*; University of Göttingen: Göttingen, Germany, 1997. (b) Sheldrick, G. M. *SHELXL 97, Program for Crystal Structure Refinement*; University of Göttingen: Göttingen, Germany, 1997.

(16) (a) Li, Y.; Zhang, H.; Wang, E.; Hao, N.; Hu, C.; Yan, Y.; Halld, D. *New J. Chem.* **2002**, *26*, 1619. (b) Shi, Q.; Cao, R.; Sun, D. F.; Hong, M. C.; Liang, Y. C. *Polyhedron* **2001**, *20*, 3287.

(17) (a) Zhang, L. Y.; Liu, G. F.; Zheng, S. L.; Ye, B. H.; Zhang, X. M.; Chen, X. M. *Eur. J. Inorg. Chem.* **2003**, 2965. (b) Nakamoto, K. *Infrared and Raman Spectra of Inorganic and Coordination Compounds*; John Wiley & Sons: New York, 1986.

(18) (a) Li, S. L.; Lan, Y. Q.; Ma, J. F.; Yang, J.; Liu, J.; Fu, Y. M.; Su, Z. M. *Dalton Trans.* **2008**, 2015. (b) Evans, H. T.; Pope, M. T. *Inorg. Chem.* **1984**, *23*, 501. (c) Maguerès, P. L.; Ouahab, L.; Golhen, S.; Grandjean, D.; Peña, O.; Jegaden, J. C.; Gomez-Garcia, C. J.; Delhaès, P. *Inorg. Chem.* **1994**, *33*, 5180.

(19) (a) Bünzli, J. C. G.; Piguet, C. *Chem. Rev.* **2002**, *102*, 1897. (b) Ghosh, S. K.; Bharadwaj, P. K. *Inorg. Chem.* **2003**, *42*, 8250.

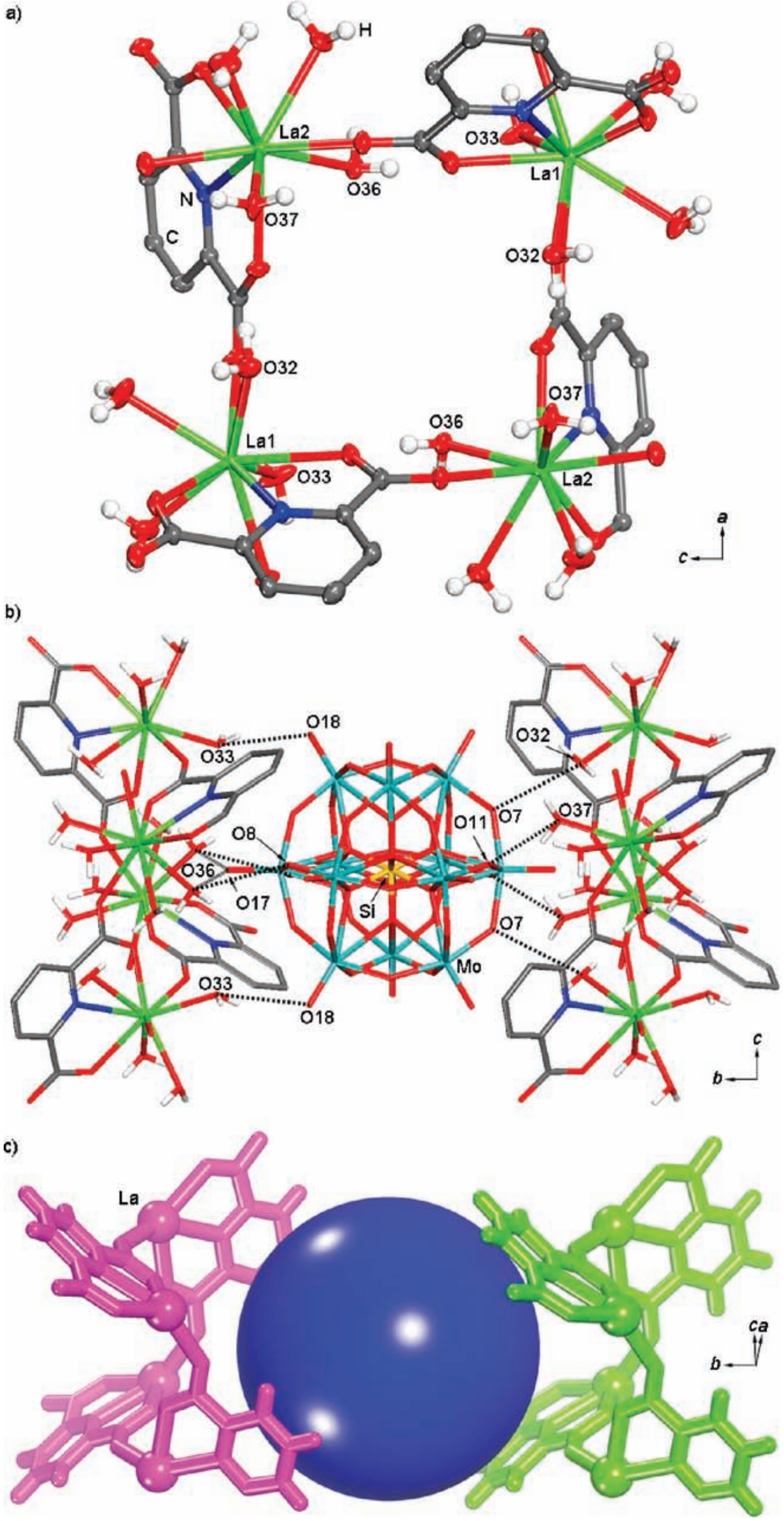

Figure 3. (a) Structure of the tetranuclear cyclic unit in compound **1**. (b) View of the hydrogen bonds between two tetranuclear cyclic units $\{[La(H_2O)_4(pdc)]_4\}^{4+}$ and $[SiMo_{12}O_{40}]^{4-}$ ions. (c) The chelate model of hydrogen bonds. The Keggin POM anions are represented as blue spheres.

O−H···O hydrogen bonding, (ii) a zeolite-like four-connected cationic network with the GIS topology, and (iii) large cavities formed by the intersected channels.

As shown in Figure 3a, four nine-coordinated La^{3+} ions are linked by carboxylate groups of four pdc ligands to form a tetranuclear cyclic unit, $\{[La(H_2O)_4(pdc)]_4\}^{4+}$. Interestingly,

Table 3. Hydrogen Bond Lengths (Å) and Angles (deg) of **1**[a]

D−H···A	d(D−H)	d(H···A)	<(DHA)	d(D···A)
O(32)−H(32B)···O(7)$^{\#1}$	0.850	2.555	170.95	3.397
O(33)−H(33A)···O(18)$^{\#2}$	0.850	2.365	139.80	3.063
O(36)−H(36B)···O(17)$^{\#3}$	0.850	2.408	170.71	3.250
O(37)−H(37B)···O(11)$^{\#4}$	0.850	2.411	142.38	3.128

[a] Symmetry codes for **1**: (#1) $x, -y+1, z+1/2$; (#2) $x, -y+2, z+1/2$; (#3) $-x+1, -y+2, -z+1$; (#4) $-x+1, -y+1, -z+1$.

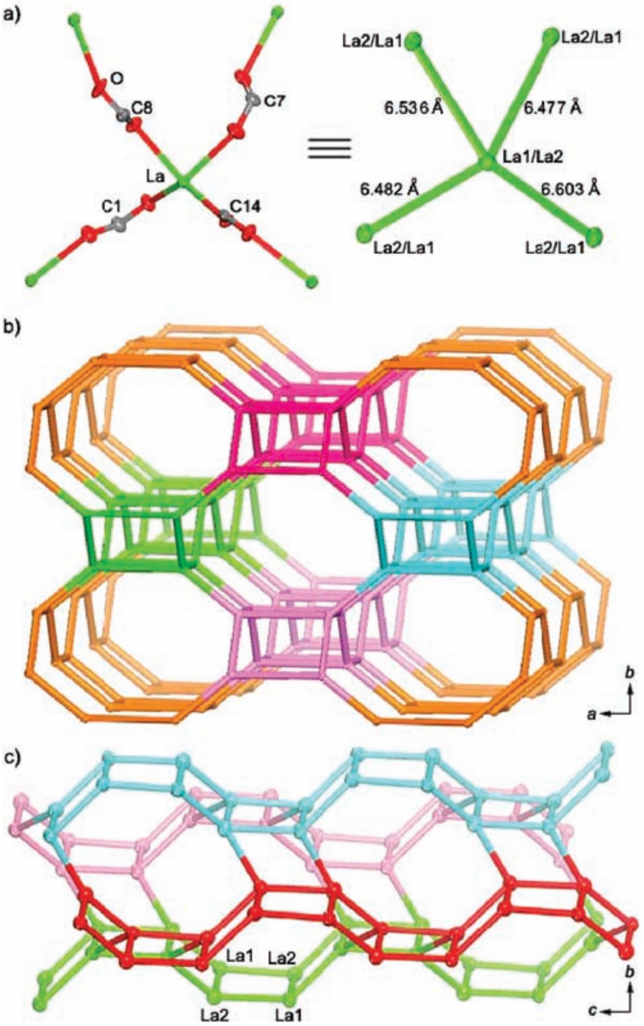

Figure 4. (a) Second building unit and its simplified sheet. (b) View of the zeolite-like four-connected 3D $4^3\cdot6^2\cdot8$ topology network along [001] direction. (c) Eight-membered channel [001] from the cc (different colors represent distinct cc's) and its cavities (also see part b).

two such tetranuclear cyclic units chelate one $[SiMo_{12}O_{40}]^{4-}$ ion through O−H···O hydrogen bonding (Figure 3b, Table 3). Simplifying the $[SiMo_{12}O_{40}]^{4-}$ ion as a sphere, an interesting chelate model is illustrated in Figure 3c. Notably, there exists an octanuclear metallamacrocycle composed of $La_8(pdc)_8$ in compound **1** (La···La nuclear-to-nuclear distance of 17.2 Å × 12.8 Å; Figure S1a of Supporting Information). A 3D lanthanide−organic cationic architecture is built up from the tetranuclear cyclic units and octanuclear metallamacrocycles (Figure S2, Supporting Information).

A remarkable structural feature of **1** is the zeolite-like four-connected cationic network with the GIS topology. As depicted in Figure 4a, each mononuclear Ln(III) center (La1 or La2 in **1**) can be regarded as a four-connected node, which is separated from other four Ln centers by the O−C−O rods. The separations of La···La are 6.482 Å, 6.536 Å, 6.477 Å, and 6.603 Å, respectively. On the basis of the four-connected nodes (Figure 4a), a 3D uninodal cationic network can be built up with Schläfli symbol of $(4^3\cdot6^2\cdot8)$, which is related to the structural prototype of natural zeolite GIS.[20,21] The four-membered rings, $\{[La(H_2O)_4(pdc)]_4\}^{4+}$, can be also treated as the unit of the double-crankshaft chain (cc). These cc chains propagate and intersect each other to form the GIS network (Figure 4b). To the best of our knowledge, lanthanide−organic coordination polymers with zeolite-like GIS topology have not been reported to date.

Generally, the formation of the inorganic zeolite architectures depends on the corner-sharing tetrahedral TO_4 (T = Si or Al). In coordination chemistry, with organic ligands as linkers and the well-defined coordination geometries of transition metals as four-connected nodes, a large number of MOFs with zeolite topological structures have been reported.[22] In contrast to transition metals, it is difficult to form the TO_4 unit of zeolites from lanthanide metals because coordination numbers of lanthanide elements are high and coordination geometries are hard to control.[23] For example, a 3D lanthanide-pdc neutral MOF $\{La_2(pdc)_3\cdot3H_2O\}$ which contains $[La(COO)_5]$ building blocks has been synthesized by Bharadwaj and Ghosh[24] but does not have zeolite topology owing to the absence of the TO_4 building unit. In our work, the introduced nanosized $[SiMo_{12}O_{40}]^{4-}$ POMs prevent La^{3+} ions from coordinating with more carboxylate groups of pdc ligands. As a result, compound **1** possesses the $[La(COO)_4]$ second building unit (SBU), which is essential for the formation of GIS-like cation framework. Therefore, the $[SiMo_{12}O_{40}]^{4-}$ ions play a crucial template role for the construction of zeolite-like lanthanide−organic cation frameworks.

Further, eight-membered channels would be found along the [001] directions in the 3D cationic network of **1** (Figure 4c). These channels intersect each other to form large cavities, which array in a zigzag fashion and are occupied by nanosized $[SiMo_{12}O_{40}]^{4-}$ counterions (Figure 5). Each large cavity could be also regarded as the assembly of the above-mentioned tetranuclear cyclic unit $\{[La(H_2O)_4(pdc)]_4\}^{4+}$ and octanuclear metallamacrocycle $La_8(pdc)_8$ (23.901 Å × 21.848 Å × 18.391 Å, nuclear-to-nuclear, measured between opposite La atoms; Figure S1b, Support-

---

(20) (a) Baerlocher, C.; Meier, W. M. *Helv. Chim. Acta* **1970**, *53*, 1285. (b) Fischer, K.; Schramm, V. *Adv. Chem. Ser.* **1971**, *101*, 250. (c) Pluth, J. J.; Smith, J. V.; Bennett, J. M. *J. Am. Chem. Soc.* **1989**, *111*, 1692. (d) Tian, Y. Q.; Zhao, Y. M.; Chen, Z. X.; Zhang, G. N.; Weng, L. H.; Zhao, D. Y. *Chem. Eur. J.* **2007**, *13*, 4146.

(21) Blatov, V. A. *TOPOS, A Multipurpose Crystallochemical Analysis with the Program Package*; Samara State University: Samara, Russia, 2004.

(22) (a) Tian, Y. Q.; Cai, C. X.; Ji, Y.; You, X. Z.; Peng, S. M.; Lee, G. S. *Angew. Chem., Int. Ed.* **2002**, *41*, 1384. (b) Tian, Y. Q.; Cai, C. X.; Ren, X. M.; Duan, C. Y.; Xu, Y.; Gao, S.; You, X. Z. *Chem. Eur. J.* **2003**, *9*, 5673. (c) Tian, Y. Q.; Chen, Z. X.; Weng, L. H.; Guo, H. B.; Gao, S.; Zhao, D. Y. *Inorg. Chem.* **2004**, *43*, 4631. (d) Li, Z.; Zhu, G.; Guo, X.; Zhao, X.; Jin, Z.; Qiu, S. *Inorg. Chem.* **2007**, *46*, 5174.

(23) (a) Kiritsis, V.; Michaelides, A.; Skoulika, S.; Golhen, S.; Ouahab, L. *Inorg. Chem.* **1998**, *37*, 3407. (b) Long, D. L.; Blake, A. J.; Champness, N. R.; Schroder, M. *Chem. Commun.* **2000**, 1369.

(24) Ghosh, S. K.; Bharadwaj, P. K. *Inorg. Chem.* **2004**, *43*, 2293.

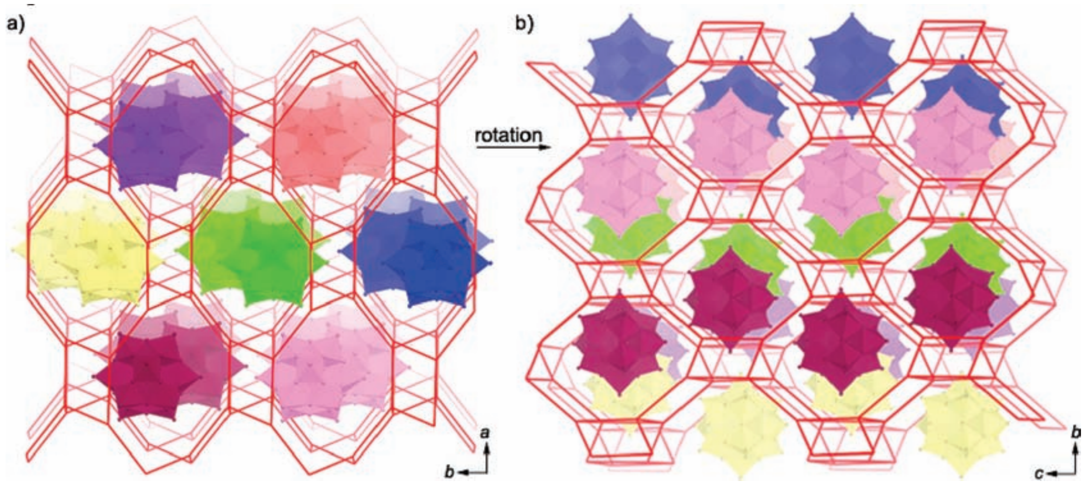

Figure 5. Cavities of intersected channels in a zigzag arrangement occupied by $[SiMo_{12}O_{40}]^{4-}$ counterions: (a) channel I, along [001] direction, and (b) channel II, along [100] direction. Polyhedrons: $[SiMo_{12}O_{40}]^{4-}$.

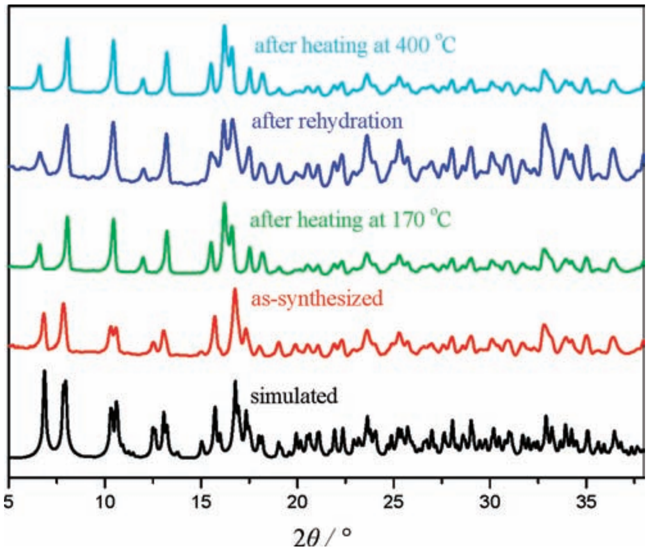

Figure 6. PXRD patterns of compound **1**.

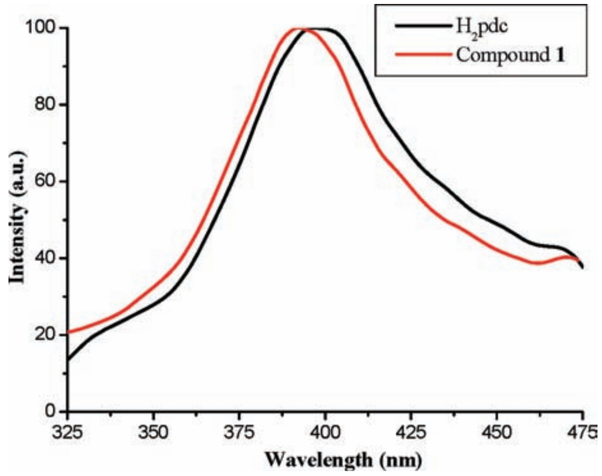

Figure 7. Emission spectra of ligand H_2pdc and compound **1** in the solid state at room temperature.

ing Information). In addition, we tried to use small anions (such as SO_4^{2-} and ClO_4^-) to exchange the anions template $[XMo_{12}O_{40}]^{4-}$ (X = Si, Ge) in compounds **1**−**6** because of the presence of channels. However, although many experiments were done, no crystal could be obtained. The investigation of crystal structures reveals that the anions $[XMo_{12}O_{40}]^{4-}$ (X = Si, Ge) are located inside the large cavities from the intersected channels, but the maximum diameter of the window of the cavity is less than that of the anions, $[XMo_{12}O_{40}]^{4-}$. Therefore, exchange of $[XMo_{12}O_{40}]^{4-}$ anions (X = Si, Ge) by other small anions could be difficult.

TG Analyses of Compounds 1−6. TG analysis of compound **1** shows a 0.96% weight loss between 40 and 80 °C which corresponds to crystallographic water (calculated value: 1.07%). From 80 to 170 °C, compound **1** loses its coordinated water, and the weight loss of 9.11% is a good accordance with the calculated value 8.58%. The 4.96% weight loss (calculated value: 4.92%) from 400 to 520 °C is ascribed to the release of one pdc molecule. Then, the decomposition of the framework compound **1** occurs starting at 520 °C. Compounds **2**−**6** exhibit similar weight loss stages (Figure S3, Supporting Information).

Powder X-ray Diffraction (PXRD). Encouraged by the single crystal X-ray diffraction results, we carried out PXRD experiments to investigate the stability of compound **1** upon the removal of free water molecules according to TG analysis. The XRD patterns indicate that the as-synthesized compound matches with the simulated one except for some intensity difference. When treated at 80 °C for 1 h, the crystal sample loses some of the lattice water molecules, and the color is still yellow. After heating at 170 and 400 °C for 1 h, respectively, the color of the sample changes from yellow to green, and the coordinated water is lost, according to TG analysis. The sample heated at 170 °C is treated in water for 12 h, and the color of the sample returns to yellow again. The XRD patterns of three samples remain essentially identical to those of the as-synthesized and simulated compound **1**, as shown in Figure 6. The slight shift and splitting of some peaks may be attributed to the subtle change of the relative positions of some atoms in the crystal lattice.[3a] This phenomenon is commonly observed in zeolites and molecular sieves, which indicates the same framework structure as that of the as-synthesized of compound **1**.[25]

Photoluminescent Properties. Compounds **1**−**6** exhibit photoluminescent properties at ambient temperature. The maximum emission peak of compound **1** is located at 392 nm upon excitation at 245 nm (Figure 7). The resemblance between compound **1** and H_2pdc implies that the luminescent behavior is ligand-based emission. However, in comparison with that of H_2pdc, the maximum emission band of compound **1** is blue-shifted. The blue-shift of emission may be attributed to the chelating of the H_2pdc ligand to the metal ion, which effectively increases the rigidity of the ligand and reduces the loss of energy by radiationless decay of the intraligand emission exited state.[26] Compounds **2**−**6** exhibit photoluminescent properties similar to those of compound **1** (Figure S4, Supporting Information).

Conclusion

In this work, we have successfully assembled six isostructural 3D POM-based lanthanide−organic coordination polymers from H_2pdc ligand under hydrothermal conditions. These compounds display a four-connected zeolite-like GIS topology templated by Keggin-type anions and exhibit photoluminescent phenomena. The zeolite-like GIS topology frameworks of these compounds are well retained below 400 °C, according to TG analysis and the XRD patterns. With hindsight, we can imagine that more types of these lanthanide−organic topology structures could be prepared by use of other organic linkers or anion templates. Further, it is reasonable to believe that the present work is important so as to expand on the application of these kinds of materials in molecular adsorption and catalysis. These efforts are currently ongoing.

Acknowledgment. This work was supported by the Natural Science Fund Council of China (NSFC, Nos. 20671011, 20731002, 20701011, 10876002, 20801005, 20801004), the 111 Project (B07012), Key Laboratory of Structural Chemistry Foundation (KLSCF, No. 060017), Basic Research Fund of Beijing Institute of Technology (Nos. 20060742022, 20070742010), China Postdoctoral Science Foundation (No. 20070410037), and the Key Project of Chinese Ministry of Education (No. 208116).

Supporting Information Available: X-ray crystallographic files in CIF format, some structural figures, X-ray powder diffraction patterns, emission spectra, and TG analyses curves. This material is available free of charge via the Internet at http://pubs.acs.org.

IC801846H

---

(25) (a) Reineke, T. M.; Eddaoudi, M.; Fehr, M.; Kelley, D.; Yaghi, O. M. *J. Am. Chem. Soc.* **1999**, *121*, 1651. (b) Du, M.; Chen, S. T.; Bu, X. H. *Cryst. Growth Des.* **2002**, *2*, 625. (c) Breck, D. W. *Zeolite Molecular Sieves, Structure, Chemistry, and Use*; John Wiley & Sons: New York, 1974.

(26) (a) Adamson, A. W.; Fleischauer, P. D. *Concepts of Inorganic Photochemistry*; Wiley: New York, 1975. (b) Zheng, S. L.; Tong, M. L.; Tan, S. D.; Wang, Y.; Shi, J. X.; Tong, Y. X.; Lee, H. K.; Chen, X. M. *Organometallics* **2001**, *20*, 5319. (c) Valeur, B. *Molecular Fluorescence: Principles and Applications*; Wiley-VCH: Weinheim, Germany, 2002. (d) Zhou, X. X.; Cai, Y. P.; Zhu, S. Z.; Zhan, Q. G.; Liu, M. S.; Zhou, Z. Y.; Chen, L. *Cryst. Growth Des.* **2008**, *8*, 2076. (e) Li, C. H.; Huang, K. L.; Dou, J. M.; Chi, Y. N.; Xu, Y. Q.; Shen, L.; Wang, D. Q.; Hu, C. W. *Cryst. Growth Des.* **2008**, *8*, 3141.